

Contents lists available at ScienceDirect

### NDT&E International

journal homepage: www.elsevier.com/locate/ndteint



# Early interferometric detection of rolling contact fatigue induced microcracking in railheads



J.J.F. van 't Oever<sup>1</sup>, D. Thompson<sup>1</sup>, F. Gaastra, H.A. Groendijk, H.L. Offerhaus\*

University of Twente, Optical Sciences Group, P.O. Box 217, 7500 AE Enschede, The Netherlands

#### ARTICLE INFO

Keywords:
Rolling contact fatigue
Optical coherence tomography
Maintenance

#### ABSTRACT

In the world of rail travel, unplanned track maintenance constitutes disruption and negatively impacts customer satisfaction. To maintain railway networks it is necessary to plan maintenance before it becomes critical, preferably by at least a year. A major concern in railway quality is the occurrence of micro-cracks in railhead surfaces, due to rolling contact fatigue. When these cracks are superficial, no more than about a millimeter in depth, the railhead lifetime can be increased by grinding or polishing. However, the deeper the cracks are, the sooner they will grow beyond a depth that can be managed by polishing. Current inspection techniques are able to detect millimeter sized cracks, but no smaller. We present a new technique for the detection of cracks in railheads, which is able to detect cracks of 20–100 µm depth optically, by way of broadband, spatially incoherent optical coherence tomography. Detection of micro-cracks at an earlier stage of development and the study of their progression will aid in advance planning and scheduling of maintenance.

#### 1. Introduction

There are currently various combinations of ultrasonic and magnetic rail inspection techniques in use (PEC and ACFM) [1,2]. When integrated into an inspection train these techniques can measure cracks with depths of 2 mm and deeper at speeds exceeding 70 km/h [3]. Cracks less than 2 mm deep go undetected for some time.

Ringsberg describes the progression of a rolling contact fatigue (RCF) induced crack in three phases [4]. Phase I involves the initiation of a crack on the rail surface due to shear stress, phase II is described as transient crack growth and phase III as tensile and/or shear-driven crack growth. Crack initiation is defined to be complete when phase I is over and the crack begins to grow further into the interior of the rail, usually at an oblique angle to the surface. At this point the surface crack is no more than  $500\,\mu m$  deep, below the detection limits of current non-destructive techniques (NDT).

Ringsberg also calculates the estimated number of wheel passages needed to initiate a RCF crack for a specific situation, as did Wickramasinghe et al. [5]. Depending on the exact mass, speed and frequency of passing trains crack initiation could be complete between 2 months to over a year after initial use of the track. It is at this point that phase II begins, during which the crack grows to a size that is large enough to be detected by traditional methods.

In another article Ringsberg describes a model to estimate the rate

of crack growth after initiation [6]. It is estimated that a 400  $\mu m$  deep crack will grow at a rate of 0.007  $\mu m$  per cycle, that is, per wheel passage. This means it will take about  $2\cdot 10^5$  cycles for such a crack to grow by 1.5 mm, into a size measurable by eddy current based techniques that are currently in use. This corresponds to about 4–5 additional months of operational time before cracks become detectable. If the surface cracks could already be detected during the earliest stages of initiation this would add at least 7 months to monitor crack progression and plan maintenance for crack mitigation.

Preventive grinding of rail is already a common practice on many networks, however without extensive knowledge of the location and level of the worst damage it is difficult to plan efficiently where to grind next and which sections of track can be left alone for a while longer. As a grinding cycle removes no more than about 300  $\mu$ m of a rail surface [7], any damage larger than this will remain as a starting point for crack growth, again reducing the useful life of the railhead. Thus a method for the more timely detection of RCF-induced surface cracking is needed to enable more informed maintenance decisions.

In this paper we describe an OCT-based optical method which can detect early stage micro-cracks by measuring single shot line profiles on railheads. A comparable, more complex OCT technique is instead able to image a full metallic surface with comparable depth resolution [8], but uses XY-scanning to achieve the surface scan.

<sup>\*</sup> Corresponding author.

E-mail addresses: h.l.offerhaus@utwente.nl (H.L. Offerhaus).

 $<sup>^{1}</sup>$  Authors contributed equally to this work.

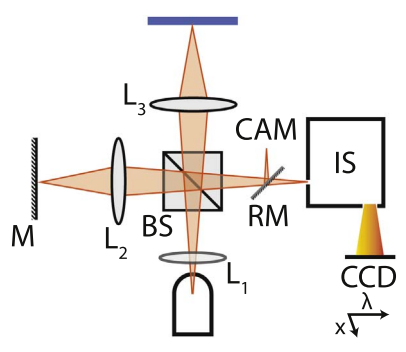


**Fig. 1.** Schematic representation of the optical setup. A vertical line on the surface of the object is interferometrically imaged onto the entrance of the imaging spectrograph, which spectrally disperses the image horizontally.

#### 2. Experimental details

#### 2.1. Setup

The system is a broadband spatially incoherent optical coherence tomography (OCT) setup. It is a combination of a wide-field Michelson interferometer, an imaging spectrograph and a camera, as shown in Fig. 1. The light sources used are a JET 660-05 power LED (Light Emitting Diode, Roithner Laser, Austria) for initial alignment and resolution measurements, and a more powerful CT-120 power LED (Luminus, USA) for the final measurements performed on rail. The JET LED has an integrated collimation lens while an external lens (L<sub>1</sub>, f=40 mm) was used with the CT-120 LED. Light from the LED is divided by a 50/50 beam splitter cube (BS) into the sample arm and the reference arm. It is then imaged onto the sample and the reference mirror  $(M_{ref})$  by a pair of identical objectives  $(L_2 \text{ and } L_3)$  with 2.5× magnification and 0.25 NA. The objectives image the sample and reference mirror surfaces onto the vertical entrance slit of the imaging spectrometer (IS, Newport 74100 with 1200 line/mm blazed grating). The image can also be diverted to a CCD camera (CAM, UEye UI-122xLE-m) using the removable mirror (RM) to take a microscope image of the measurement region. The imaging spectrograph images the entrance slit onto the CCD camera (Basler Ace acA3800-14um), while spectrally dispersing the line along the horizontal axis, thus yielding a spectrum for each position on the entrance slit.

Images from the sample and reference surfaces are spatially coherent as light is coherently divided and recombined by the beam splitter. These images are superimposed on the entrance slit, which slices out a thin vertical line, discarding the rest of the image. Each point along this line corresponds with one position on the sample and on the reference mirror. By measuring and analyzing the spectrum at each point we can calculate the height profile along the line on the sample. The spectra at all points are captured by the CCD in a single frame, allowing single-shot measurement of the height profile along a line on the sample.

The intensity on the CCD at the output of the spectrograph can be described as

$$I(x, \lambda) = S(\lambda) \left( c(x) + a(x) \cos\left(\frac{2\pi D(x)}{\lambda}\right) \right), \tag{1}$$

with  $S(\lambda)$  being the spectrum of the light source, x the position along the line, c(x) an offset related to the relative intensities returning from the sample and reference arm, a(x) the amplitude of the oscillation and D = 2h(x) the optical path length difference (OPD), with h(x) being the height profile on the sample relative to the flat reference mirror [9].

As an example, a simulated height profile and the corresponding image on the CCD can be seen in Fig. 2. It is calculated using formula (1) using S and a equal to one, c set to zero and an observable spectral range of 16.8 nm, which is typical for the light sources used in this work. The figure shows how different heights h encode into different

periodicities and phase shifts. Light from a LED is spatially incoherent and therefore crosstalk between spectra recorded for adjacent positions is very low [10].

The theoretical lateral resolution, based on the NA of the objectives, is 4.5  $\mu$ m [11]. In typical OCT, the depth resolution  $\Delta h$  depends on the spectral width of the light source as

$$\Delta h = \frac{2\ln(2)\lambda_0^2}{\pi\Delta\lambda},\tag{2}$$

with  $\lambda_0$  being the central wavelength and  $\Delta\lambda$  the full width at half maximum intensity (FWHM) [12]. However, in our case we have only a single reflection coming from the sample. The depth resolution is therefore limited only by the error in the determination of the fringe frequency and phase. Two important factors are the pixel signal-tonoise ratio and fringe visibility, which depends on sample reflectivity. The length of the imaged line is 1.4 mm and is currently limited by the CCD chip dimensions.

#### 2.2. Data processing

Each frame is processed line by line along the spatial axis (for each position x). The fringe pattern for each position is first normalized to the spectrum by dividing by an 8th order polynomial fit. Next, the offset c and the amplitude a are determined from the dc-component and largest non-dc-component of the Fourier transform of the normalized pattern, respectively. Lastly, the OPD is determined by comparing the normalized pattern to formula (1) using a range of trial values for D (in  $1 \mu m$  steps) and  $S(\lambda) = 1$ . The value of D that produces the smallest absolute difference with the fringe pattern is chosen as the best fit. The fringe visibility, a measure of signal strength, is then determined as the ratio of a to c. If the visibility falls below 1% the fit is no longer deemed reliable and the extracted OPD value is not used. Finally the height profile is calculated as h(x) = D(x)/2.

#### 3. Results

#### 3.1. Determination of lateral and depth resolution

To determine the lateral resolution, we image a test sample with reflective lines and determine the smallest line width which is still properly resolved, corresponding to the spatial cut-off frequency of the modulation transfer function of the optical system [11]. The test sample consists of a lithography mask containing arrays of reflective chromium lines on a glass substrate. The width of the lines is different for each array and varies logarithmically from  $1\,\mu m$  to  $50\,\mu m$  in 20steps. The side-to-side line separation is equal to the line width, creating a square periodic pattern with 50% duty cycle. The test sample is placed in the sample arm of the interferometer, the reference arm is blocked and for each periodic pattern a line image is recorded using the CCD behind the spectrograph. The visibility of the periodic patterns is calculated using  $(I_{max} - I_{min})/(I_{min} + I_{max})$  with  $I_{max}$  and  $I_{min}$  the measured intensity from a reflective and non-reflective part of the pattern, respectively. The lateral resolution is taken to be the smallest line width with a visibility larger than 1/e (approximately 37%) of the maximum visibility. The measurement results are shown in Fig. 3. The maximum visibility is approximately 17.5% and the lateral resolution found is 8 µm.

To determine the depth resolution a purely reflective part of the calibration sample was measured while placed at an angle 1.83° relative to the reference mirror, leading to an increasing OPD along the line. The height profile was measured and a linear function was fitted using the least squares method. Both the profile and the profile minus the linear fit  $h^*$  is shown in Fig. 4. The standard deviation of the  $h^*$  profile is  $\sigma=0.94~\mu m$  and the depth resolution calculated as  $2\sigma$  equals  $1.9~\mu m$ .

## Download English Version:

# https://daneshyari.com/en/article/4925181

Download Persian Version:

https://daneshyari.com/article/4925181

<u>Daneshyari.com</u>